Received: 1 October 2021 | Revised: 26 January 2022 | Accepted: 4 March 2022

DOI: 10.1002/app.52408

ARTICLE

Applied Polymer SCIENCE WILEY

Transamidation-based vitrimers from renewable sources

Luca Pettazzoni | **Francesca Leonelli** | **Andrea Martinelli** | **Luisa Maria Migneco** | **Sara Alfano** | **Daniele Di Luca** | **Lorenzo Celio** | **Valerio Di Lisio**

Department of Chemistry, Sapienza Università di Roma, Rome

Correspondence
Luca Pettazzoni, Department of Chemistry, Sapienza Università di Roma, Piazzale Aldo Moro 5, 00185, Rome, Italy.
Email: luca.pettazzoni@uniroma1.it

Abstract

Vitrimers are polymeric materials that behave as thermosets at room temperature but, when heated, they exhibit a plastic flow similar to thermoplastics, enabling their reprocessability. A series of new bio-based polyamide-polyamine *vitrimers* are synthetized starting from tris(2-aminoethyl)amine and epoxidized methyl oleate, a material that can be easily prepared from renewable resources obtainable both from natural products and waste. The incorporation of free amine groups in the network enables the transamidation exchange reaction with the crosslinking amide functions; this reaction, if appropriately catalyzed, donates a full reprocessability to the material. Boric acid, which is known to be a green, cheap and non-toxic catalyst for transamidation reactions, is employed in this work. Once that the optimal condition for the transamidation reaction is found, different catalyst loadings are tested and the obtained materials are subjected to thermal and mechanical characterization. The obtained materials possess good thermal stability up to 300°C and a T_g value ranging between 7 and 21°C depending on the $B(OH)_3$ content. Furthermore it is possible to observe how the introduction of boric acid in the materials reduces the E_a (inferred from stress-relaxation experiments) of the transamidation reaction from 130 ± 8 KJ mol^{-1} to a mean value of 63 ± 4 KJ mol^{-1}.

KEYWORDS

biopolymers and renewable polymers, catalysts, polyamides, recycling, stimuli-sensitive polymers

1 | INTRODUCTION

Polymeric materials are usually classified in two main groups: thermoplastics and thermosets. Thermoplastics are formed by linear polymeric chains held together by non-covalent interactions, such as hydrogen bonds or Van der Waals interactions.[1] These materials possess the ability to flow upon heating, making it possible to reprocess them multiple times, but their mechanical and thermal properties as well as the chemical resistance are different and, possibly, inferior compared to that of thermosets.[2] The latters, in fact, consist of a cross-linked structure, completely made up of covalent bonds. The 3D network structure can confer to amorphous polymers at temperature above the glass transition elastomeric behavior or, according to the macromolecules chemical

features and cross-linking density, high stiffness, thermal and chemical stability.[3] Nevertheless, due to the presence of inter-chain covalent cross-links, thermosetting materials are not reprocessable and, then, not recyclable. At the end of usage, they are sent to landfill, to incineration plants for energy recovery or employed as secondary raw material for production of low added value items, which are all environmentally or economically impactful procedures. In the last years, a new category of materials gained a position between thermoplastics and thermosets: this new class has been named Covalent Adaptable Networks (CANs) by Bowman et al. in 2010.[4] These can be described as the species that bridges the gap between thermoplastics and thermosets. In fact, they are formed by a covalent 3D network (like thermosets) in which, as a result of a determinate stimulus, some of the cross-links can be dynamically broken and re-formed or undergo an exchange reaction, leading the material to become viscous (like thermoplastics).[5] Hence, CANs possess the mechanical and chemical properties of thermosets but, at the same time, can be recycled, reprocessed and could show self-healing ability.

Covalent adaptable networks are usually classified into two different categories, depending on how the density of cross-links changes following the stimulus application. The first type, named *dissociative*, presents a variable cross-links density. Once the stimulus is applied, a dissociation of the cross-links causes a partial or total depolymerization.[6] One of the first and most important example of dissociative CANs has been reported by Wudl et al., who used reversible Diels-Alder cross-linking reaction between furan and maleimide.[7] Since 2005 a multitude of reactions have been employed successfully for dissociative CANs synthesis, including radical exchange of alkoxyamines, disulphide metathesis, thiol-Michael reaction and bulky urea's bond dissociation to give isocyanates and amines.[8–11]

The other type of CANs is named *associative* and presents a fixed cross-link density, since there is a bond-forming process prior to the bond-breaking, resulting in a dynamic and fast exchange that softens the material when the stimulus is applied. Since the process is isenthalpic (network functionality is the same before and after the exchange), associative CANs behavior depends solely on the kinetic of the exchange reaction, and a catalyst is often required to provide a good reprocessability. Originally, associative CANs were based on a radical exchange mechanism but, despite the interesting results obtained in self-repairing and reprocessability, the applicability of these material was limited because of unwanted termination reactions.[5,12–14] In 2011, the concept of associative CANs has been expanded by the introduction of *vitrimers*, operated by Leibler et al.[15] In their work the authors have obtained an elastomeric epoxy network, cross-linked through esters moieties and containing free hydroxyl functions that, thanks to the presence of a catalyst ($Zn[OAc]_2$), underwent transesterification reaction at high temperatures. The resulting material had an Arrhenius-like viscosity variation with temperature; this behavior is the main characteristic of *vitrimers*, which are associative CANs, in which the exchange process is solely thermally activated. Since then, *vitrimers* have received plenty of attention, with an increasing number of reactions employed in the cross-links exchange processes, including imines/amines exchange, olefins metathesis, transthioesterification, transcarbamoylation, transamination of vinylogous urethanes, disulphides exchange and transcarbonation.[3,9,16–26] Despite the wide variety of reported exchange reactions, to the best of our knowledge there is just one work dealing with transamidation-based CANs.[27] In fact, amides are well known to be the most stable among the carboxyl derivatives, due to the delocalization of the nitrogen lone pair and, then, the required harsh conditions limit the use of transamidation as exchange reaction in CANs synthesis. In the only transamidation-based CANs example found in literature, acetoacetyl formed amides have been used as dynamic covalent bonds because of the high reactivity compared to traditional amides.

Besides the pure scientific interest for this new class of polymeric materials, there is also an environmental interest for CANs since they can be recycled, even though they are cross-linked. In this regard, according to PlasticsEurope, in 2018 the global plastic production reached 359 million tons (with a recycling percentage of just 9%) and thermosets consist of more than 20% of the annually used polymers.[27] Even though almost the entire plastic production is based on non-renewable feedstocks, in the last years many efforts have been made to move towards a more sustainable management of the resources. This results in a shift towards the use of renewable feedstocks, including vegetable oils, lactic acid, lignin (and more) instead of oil. Moreover, with the growing interest for the concept of circular economy, the use of waste as a resource has caught on thanks to the twofold benefit of the wastage production decrease and the limitation of resources squandering. On these grounds is the present research based, in which the synthesis of one of the first transamidation-based CAN with the use of renewable or waste-obtainable feedstocks is reported. In fact, the methyl ester of oleic acid (methyl [Z]-octadec-9-enoate), the most common monounsaturated fatty acid in nature, was employed as starting material. Oleic acid can be found as a component of the triglycerides present in most of vegetable oils like olive oil (71%), peanut oil (67%), high oleic sunflower oil (64%) and canola oil (60%).[28,29] Moreover, it is present in waste cooking

oil (WCO), in inedible animal fats and is one of the major component of triglycerides of olive mill wastewaters.[30–34] The possible use of these wastes not only provides new feedstocks but also solves the disposal and environmental problems deriving from their high polluting properties (one liter of WCO is estimated to contaminate one million liters of water) and large production (16,5 million tons per year).[35,36] For example, these problems have been partially solved by using WCO as a source for biodiesel production.

In the present research, polyamide-polyamine *vitrimers* (EMO-TREN) were obtained by crosslinking epoxidized methyl oleate (EMO) with tris(2-aminoethyl)amine (TREN). A ionic liquid (1-methylimidazolium tetrafluoroborate, $[Hmim]^+$ BF_4^-) was used to facilitate the epoxide ring opening by the amine function and boric acid was employed as highly efficient, low cost and eco-friendly catalyst for transamidation.[37] According to Nguyen et al., $B(OH)_3$ plays the double role of Lewis acid (with the boron atom) towards the carboxylic oxygen and of H-bond donor (with the —OH functions) towards the nitrogen of the amide.[38] The effect of different concentration of boric acid on synthetized EMO-TREN properties as well as reprocessability were evaluated. All the samples were subjected to FTIR spectroscopy, thermogravimetric (TGA), differential scanning calorimetry (DSC), dynamic mechanical (DMA) analyses as well as swelling and tensile tests, carried out before and after broken specimen healing and on specimens obtained from reprocessed films.

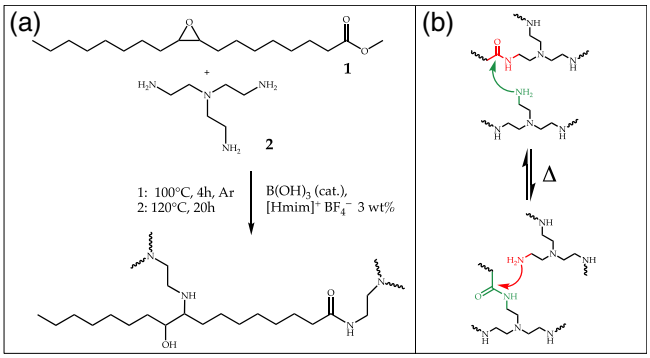

FIGURE 1 EMO-TREN polymerization (a) and transamidation exchange reaction (b) [Color figure can be viewed at wileyonlinelibrary.com]

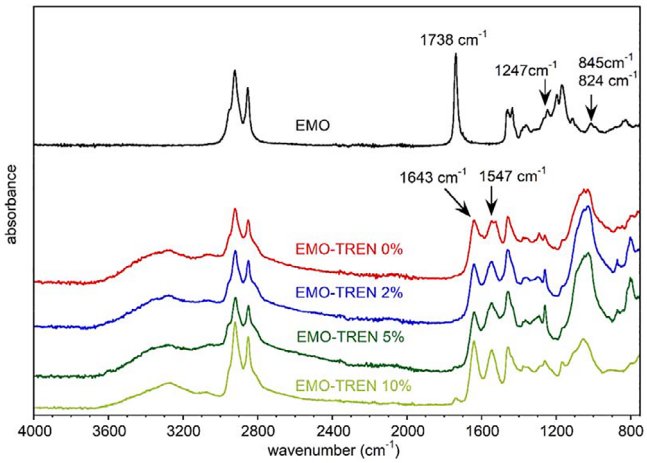

FIGURE 2 ATR-FTIR spectra of EMO and EMO-TREN with 10 Mol %, 5 Mol %, 2 Mol%, 0 Mol% loading of boric acid [Color figure can be viewed at wileyonlinelibrary.com]

2 | RESULTS AND DISCUSSION

2.1 | Synthesis of EMO-TREN networks

In order to ensure the reactant homogenization, the cross-linked polyamide-polyamine EMO-TRENs networks were prepared by pre-polymerizing epoxidized methyl oleate (EMO, **1**) and tris(2-aminoethyl)amine (TREN, **2**) in a 1 to 1 ratio (Figure 1a). The obtained homogeneous viscous liquid was then cured in a vial or in a Teflon mold at 120°C for 20 h. Choosing a 1:1 ratio between EMO and TREN leads to an excess of amines with respect to the epoxide and ester functions, leading to free amines in the network capable of the transamidation reactions. The addition of a catalytic amount of 1-methylimidazolium tetrafluoroborate ($[Hmim]^+$ $BF4^-$) allows the epoxide ring opening, that is known to be difficult in the case of internal epoxides.[39] The presence of $B(OH)_3$ (catalyst) is necessary to catalyze the transamidation exchange reaction, reported in Figure 1b.

The cross-linking reaction between epoxy and amine groups was verified by comparing the FTIR spectra of EMO and EMO-TREN samples, reported in Figure 2. The spectrum of EMO shows the bands at 1738 cm^{-1}, due to C═O stretching of esters functions, and at 1247, 845, 824 cm^{-1} of epoxide group. In the spectra of EMO-TREN all these absorptions are no more present while the bands at 1643 and 1547 cm^{-1}, due to C═O stretching and the N—H bending of the amide group, respectively, appear. Moreover, the broad signal at 3200–3500 cm^{-1}, is assigned to N—H as well as to the O—H stretching generated by the epoxide ring opening.

The broad bands of boric acid at about 3150 and 1400 cm^{-1}, due to O—H and B—O stretching, respectively, are superimposed to EMO-TREN absorption and cannot be distinguished. On the other hand, the narrow band at 1180 cm^{-1}, due to in-plane B—O—H bending, can be observed as a resolved peak only in the EMO-TREN 10% spectrum because of the higher $B(OH)_3$ concentration in the sample.[40]

2.2 | Swelling tests

The swelling tests in THF, CH_2Cl_2 and MeOH were performed to establish the cross-linked nature and the chemical resistance of the polymers synthesized with various $B(OH)_3$ loadings. The results are reported in Table 1.

The small values of the gel fractions (equal to 1.0 or 0.9 for all the tested solvents) indicate the obtainment of densely cross-linked polymers with a high chemical resistance towards the tested solvents. The samples show a higher tendency to swelling as the dielectric constant of the employed solvent is increased.

TABLE 1 SR (wt/wt) and GF (wt/wt) of EMO-TREN samples in THF, CH_2Cl_2 and MeOH

Sample		THF	CH_2Cl_2	MeOH
EMO-TREN 0%	SR	0.9	1.7	3.7
	GF	1.0	1.0	0.9
EMO-TREN 2%	SR	1.0	1.6	3.6
	GF	1.0	1.0	0.9
EMO-TREN 5%	SR	0.7	1.6	2.8
	GF	1.0	1.0	1.0
EMO-TREN 10%	SR	0.7	1.3	1.0
	GF	1.0	1.0	1.0

Abbreviations: GF, gel fraction; SR, swelling ratio.

2.3 | Thermogravimetric analysis and different scanning calorimetry

Thermogravimetric analysis was carried out to investigate thermal stability of the EMO-TREN samples in anticipation for the programmed thermal treatments used in DMTA analyses and healing experiments. Figure 3 shows the TGA (a) and the derivative (DTGA) (b) curves of EMO-TREN samples with various catalyst contents, obtained from room temperature up to 500°C under nitrogen flow. The weight loss of $B(OH)_3$, occurring between 100 and 180°C could not be observed because of its low concentration.[41]

Figure 3a shows that all samples progressively lost about 5%–10% of weight up to about 300°C, presumably because of residual methanol in the network bulk or unreacted substance traces. At higher temperatures EMO-TRENs begin to decompose by a more or less clear double weight loss, well evidenced in DTGA profiles of Figure 3b.

Neither the temperature nor the weight loss of the first decomposition process are related to sample composition, while the temperature at the maximum decomposition rate (T_d^{max}), determined from the minimum of DTGA curves, increases significantly with the addition of boric acid (Table 2**)**. This effect could be due directly to the well-known thermal stabilization activity of $B(OH)_3$ or, indirectly, to its influence on the polymer network structure.

According to TGA results, all the thermal treatments to which the sample were subjected for dynamic mechanical analysis and healing experiments were carried out at temperatures lower than those of the degradation processes onset.

The thermal properties of EMO-TRENs were investigated by DSC analysis. The thermograms, displayed in Figure 4, were recorded on pristine samples (solid lines) and after the thermal treatment at 140°C for 2 h (dashed lines), used to heal the broken samples in mechanical

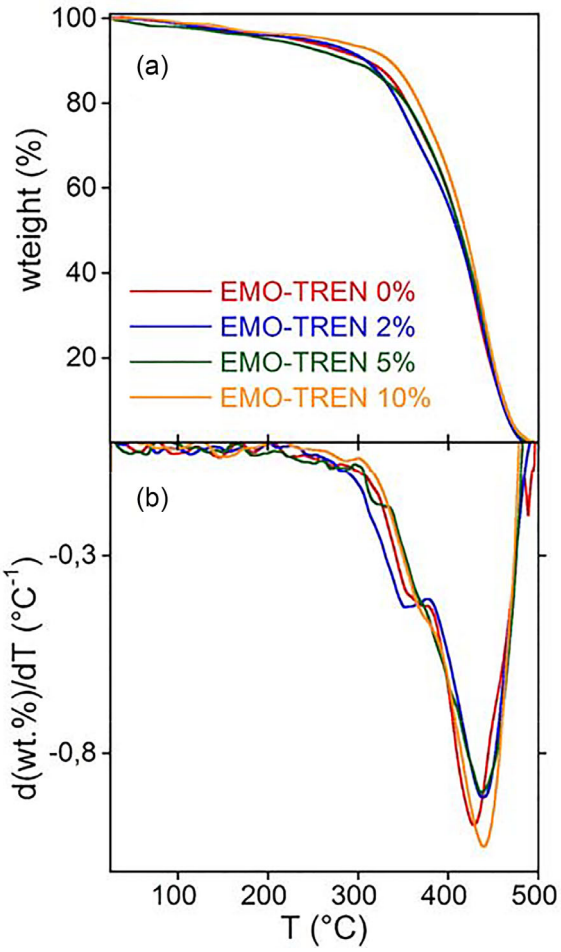

FIGURE 3 TGA (a) and DTGA (b) curves of EMO-TRENs [Color figure can be viewed at wileyonlinelibrary.com]

experiments. In the explored temperature range, all samples show only a glass transition, due to the amorphous nature of the networks. The sample without or with the lower boric acid content shows the T_g values below room temperature, at about 7–8°C (Table 2). Then, at the

TABLE 2 Thermal properties of EMO-TREN samples

		Pristine		Healed	
Sample	T_d^{max} (°C)	T_g (°C)[a]	ΔC_p (J g^{-1} K^{-1})[a]	T_g (°C)[a]	ΔC_p (J g^{-1} K^{-1})[a]
EMO-TREN 0%	428	8 ± 2	0.55 ± 0.05	11 ± 2	0.54 ± 0.03
EMO-TREN 2%	438	8 ± 3	0.64 ± 0.05	11 ± 2	0.60 ± 0.02
EMO-TREN 5%	437	7 ± 2	0.60 ± 0.02	12 ± 1	0.62 ± 0.03
EMO-TREN 10%	438	21 ± 2	0.44 ± 0.02	21 ± 2	0.49 ± 0.04

Note: T_g and ΔC_p were measured before (pristine) and after the healing process (healed).
[a]Mean value ($n = 3$; ±SD).

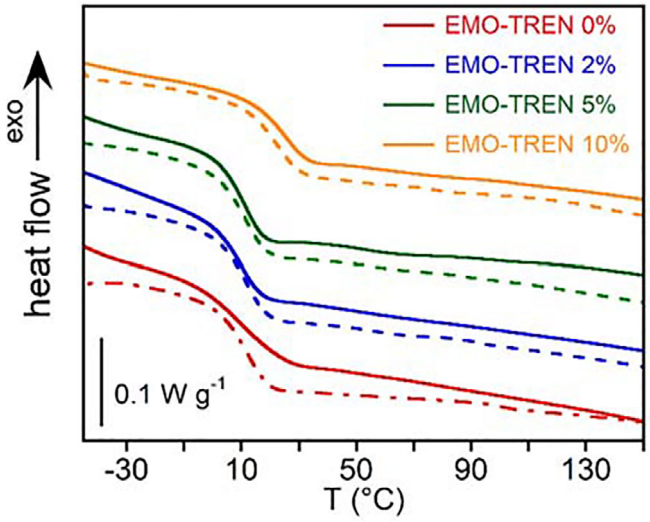

FIGURE 4 DSC curves of pristine (solid line) and reprocessed (dotted line) EMO-TRENs [Color figure can be viewed at wileyonlinelibrary.com]

highest $B(OH)_3$ concentration, the glass transition increases up to 21°C. Moreover, EMO-TREN 10% shows a specific heat capacity change (ΔC_p) at the T_g significantly lower than those of the other samples. These finding could be due to the possibility of catalyst molecules, at the highest concentration, to form inter-chain hydrogen bonds, which leads to a network mobility reduction.

In comparison to the pristine samples, the EMO-TREN specimens subjected to a further thermal treatment at 140°C for 2 h (dotted lines in Figure 4) show only a small T_g increase and a nearly equal ΔC_p (Table 2), evidencing that the healing process did not greatly affect the thermal properties of the samples.

2.4 | DMA results

The visco-elastic behavior of EMO-TRENs sample was investigated by dynamic mechanical thermal analysis from room temperature up to 150°C to locate the temperature range of the rubbery plateau. Then, stress-relaxation experiments were carried out in isothermal conditions at different temperatures within the selected range.

The variation of elastic modulus (E') and tan δ of EMO-TREN samples is reported as a function of temperature in Figure 5.

The E' and tan δ decrease at the lower temperature range, shown by all the samples, represents the tail of the α relaxation at the glass transition, starting below room temperature. After the transition completely took place, all the samples show the rubbery plateau, where the E' values remain nearly constant. Moreover, it can be observed that the elastic modulus is higher the higher the $B(OH)_3$ content is. The stress relaxation experiments were carried out in isothermal conditions at different temperatures chosen in the rubbery plateau range. The obtained normalized relaxation moduli $\frac{G(t)}{G_0}$ are reported as a function of time in Figure 6.

The characteristic relaxation time (τ), taken at $\frac{G(t)}{G_0} = \frac{1}{e} = 0.37$, of all the EMO-TRENs was reported in the Arrhenius plot of Figure 7a, which shows that the data are linearly correlated. From the slope values of the interpolating straight lines, the activation energy (E_a) for the viscous flow was calculated. In Figure 7b, E_a as a function of boric acid molar concentration is reported.

Figure 7b shows that the addition of boric acid clearly decreases the activation energy of the reaction from 130 ± 8 KJ mol^{-1} to a mean value of 63 ± 4 KJ mol^{-1}. Since the transamidation is the responsible of cross-links exchange and, then, of the sample viscous flow, the E_a found in stress relaxation experiments reflects that of the reaction. In literature few works about the synthesis of associative CANs based on transamidation are reported, being the exchange reaction with a free amine hampered by the amide bond stability. However, it has been observed that reactive amides, such as acetoacetyl formed amides, can undergo exchange reaction without catalyst and can be used for CAN preparation. In the cited work, an activation energy of 60 KJ mol^{-1} has been determined

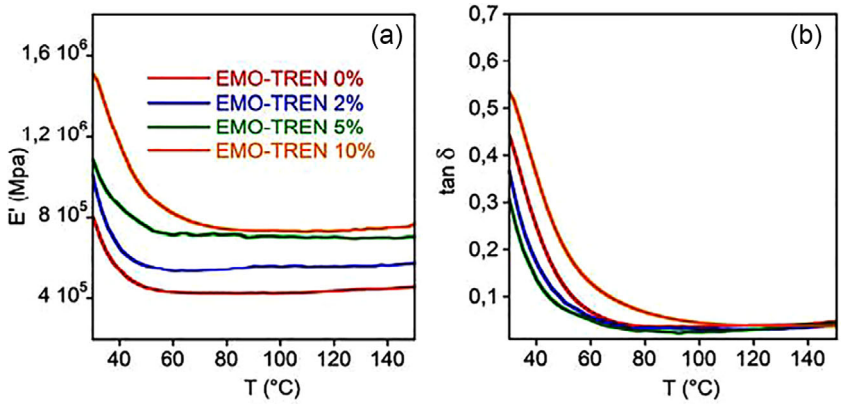

FIGURE 5 Dynamical mechanical thermal analysis. Variation of elastic modulus E' (a) and tanδ (b) of EMO-TREN samples as a function of temperature [Color figure can be viewed at wileyonlinelibrary.com]

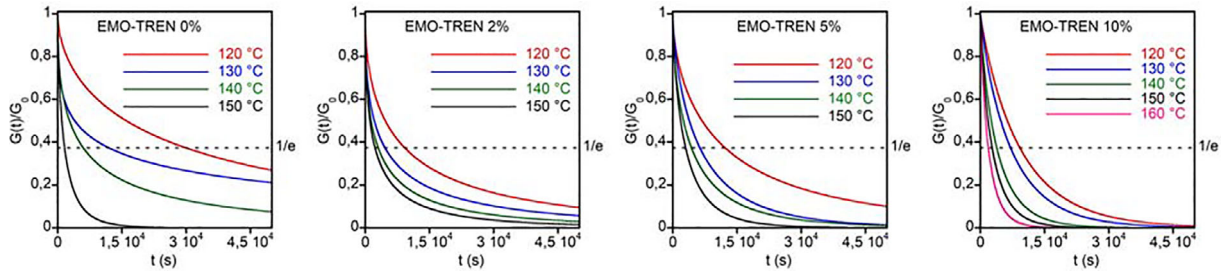

FIGURE 6 Stress-relaxation of EMO-TRENs [Color figure can be viewed at wileyonlinelibrary.com]

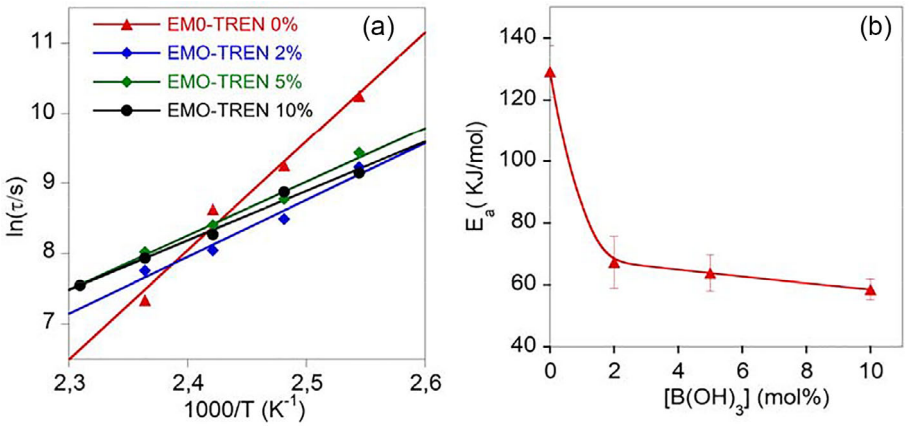

FIGURE 7 Arrhenius plot of relaxation times (t) determined at $\frac{G(t)}{G_0}=\frac{1}{e}$ with linear fit (a). Activation energy (E_a) for the viscous flow determined from the slope of the linear fit, as a function of the boric acid concentration (b) [Color figure can be viewed at wileyonlinelibrary.com]

from stress-relaxation experiments.[42] This value is very similar to those found by using low molecular weight model compounds.[42] As expected, in EMO-TRENs networks, the activation energy of the reaction involving poorly reactive amides is high but substantially decreases by the use of boric acid as catalyst. However, for the discussion of the following results about EMO-TRENs mechanical properties, it is important to remark that the $B(OH)_3$ concentration has not a marked effect on the relaxation rate. In fact, the relaxation time recorded at a fixed temperature did not significantly vary as a function of the catalysts content (Figure 7a). This means that the catalytic activity reached the maximum value already at the lower boric acid concentration.

2.5 | Tensile tests

The EMO-TRENs samples for the mechanical properties experiments were synthetized directly in the dumb-bell shaped mold. The stress–strain tests were carried out at 5 mm/min at 23°C up to the sample break, then the fracture's extremities were put in contact and the samples were heated at 140°C for 120 min in the mold (healing). The stress–strain curves of pristine and healed samples are reported in Figure 8a,b, from which Young modulus (E_Y), tensile strength and strain at break were determined and displayed in Figure 8c–e, respectively.

All the samples show that the strain rises monotonically with the deformation, being at room temperature

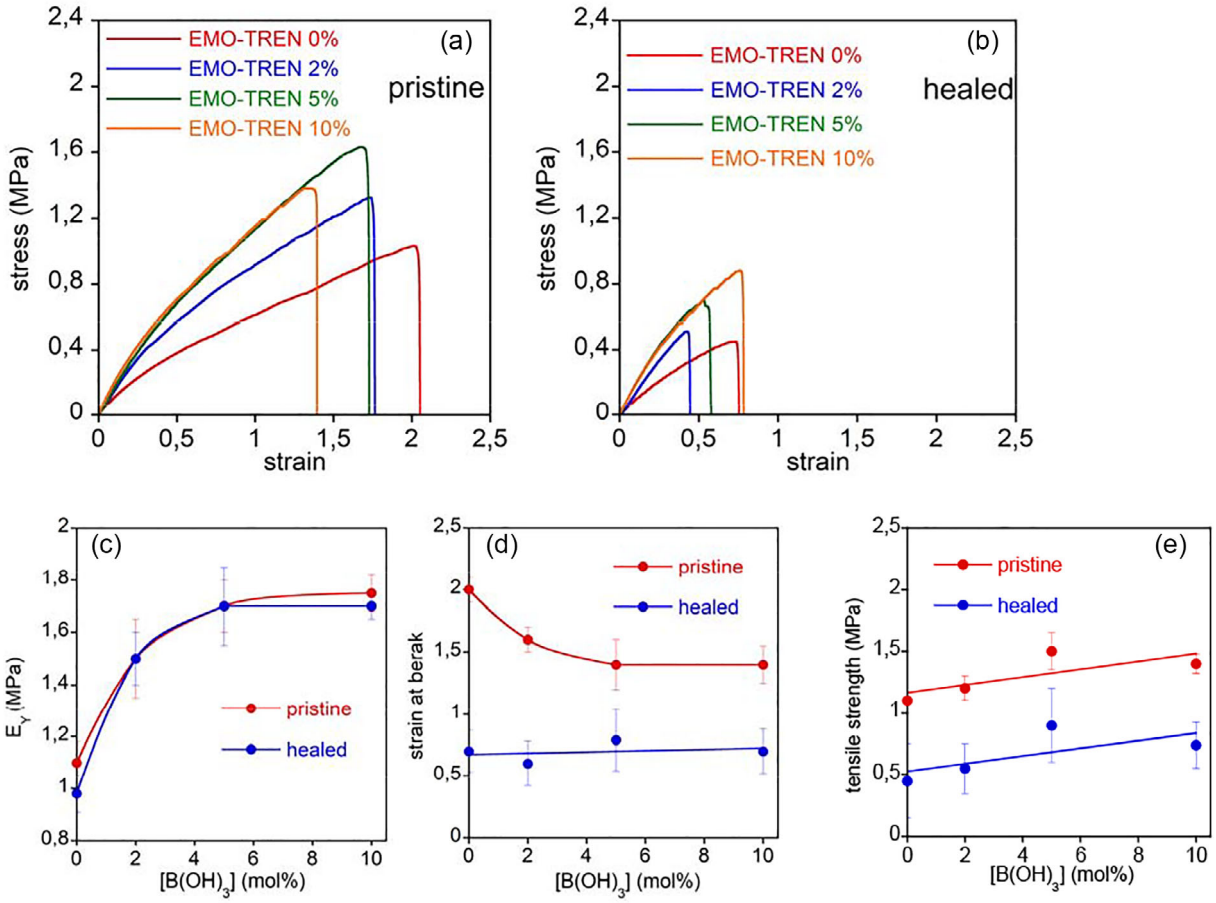

FIGURE 8 Mechanical characterization. Stress–strain curves of pristine (a) and healed (b) samples. Young modulus (E_Y) (c), strain at the break (d) and tensile strength (e) of pristine and healed samples. In figure (a–c) the curves are guides for the eyes [Color figure can be viewed at wileyonlinelibrary.com]

the chain viscous flow completely blocked by cross-links (Figure 8a). Moreover, the increment of $B(OH)_3$ brought about an overall sample rigidity, as shown by the increase of the Young modulus, a slight increase of tensile strength and a reduction of the elongation at the break (Figure 8c–e).

The second stress–strain experiment shows that the Young moduli of all EMO-TREN samples were not affected by the healing, remaining unchanged with respect to those of the pristine samples. On the other hand, a clear reduction of the tensile strength and elongation at break can be observed. As far as this evidence, a visual inspection of the broken healed samples revealed that the second failure, occurring in the same position of the first one, was prematurely triggered by small crevices, derived from imperfect coupling of the sample surfaces. However, the healing process results effective for moderate deformation.

The results of the stress relaxation experiments showed that the concentration of the catalyst had not a significant effect on the activation energy, as expected, as well as on the relaxation rate. This lets presume that the lowest $B(OH)_3$ concentration is sufficient to effectively catalyze the transamidation reaction. On the other hand, the dependency of the thermal and mechanical properties of EMO-TRENs on the amount of boric acid in the network lets infer that this molecule acts also as a reinforcing filler, setting up Supplementary non-covalent interactions through the formation of inter-chain hydrogen bonds. This double role of catalyst and filler offers the opportunity to modulate the EMO-TRENs thermal and mechanical properties by the proper choice of $B(OH)_3$ concentration.

2.6 | Reprocessability test

Two reprocessing cycles were conducted on EMO-TREN 5% by grinding the material in small pieces and placing them in a hot press, at 140°C for 3 h, under a pressure of 98 MPa. The obtained films were homogeneous and smooth at a visual inspection. In Figure 9a,b are reported

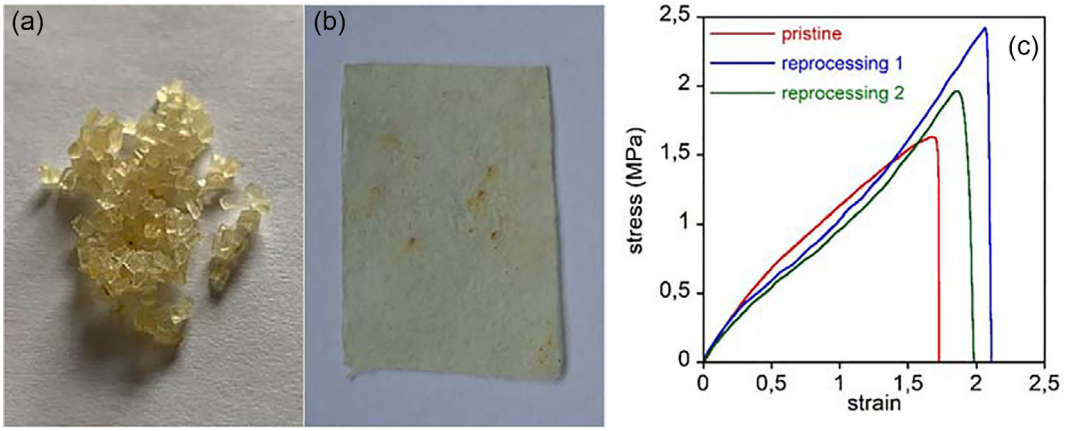

FIGURE 9 EMO-TREN 5% before (a) and after (b) first reprocessing cycle. Stress–strain curves of pristine EMO-TREN 5% sample and after the 1° and 2° reprocessing cycle [Color figure can be viewed at wileyonlinelibrary.com]

TABLE 3 Mechanical properties of EMO-TREN 5% before and after the first and second reprocessing cycles

EMO-TREN 5%	Young modulus (MPa)	Tensile strength (MPa)	Strain at break
Pristine	1.7 ± 0.1	1.5 ± 0.2	1.4 ± 0.2
Reprocessing cycle 1	1.4 ± 0.2	2.3 ± 0.2	2.3 ± 0.2
Reprocessing cycle 2	1.3 ± 0.2	2.0 ± 3	1.9 ± 0.3

the images of the grinded pristine sample and of the film obtained after the first reprocessing cycle, respectively.

Dumbbell shaped specimens were die-cut from the reprocessed films and subjected to mechanical tests. In Figure 9c, selected stress–strain curves obtained after the first and second reprocessing cycle are reported in comparison with that of a pristine sample, already displayed in Figure 8a.

The plot shows that the mechanical properties of the reprocessed films were lightly different from the original sample. In fact, in the lower strain range, the reprocessed samples behaved more compliant whereas, at the higher deformation, a stress-hardening occurred.

The analysis of the results, reported in Table 3, showed that the Young modulus decreased slightly while the tensile strength and strain at break increased.

This could be due to the reduction of the material inhomogeneities and defects which triggered the breaking process of the pristine and, mainly, of the healed samples. The results showed that the transamidation reaction, in addition to healing, confers to the materials good reprocessability properties.

3 | CONCLUSIONS

In this work one of the first transamidation-based *vitrimer* has been synthesized through the cross-linking of a renewable monomer (methyl oleate epoxidized) with tris(2-aminoethyl)amine. The insertion of a green catalyst like boric acid in the network allows to exploit the transamidation reaction that donates the *vitrimeric* behavior, confirmed by stress-relaxation experiments that permitted to obtain the activation energies for the different catalyst loadings. Changing the amount of $B(OH)_3$ also affects some of the thermal properties of the EMO-TREN, probably because boric acid acts not only as a catalyst but also as a reinforcing filler. All the synthesized materials possess good thermal stability, solvent resistance, mechanical properties and can be reprocessed by hot-pressing, even with the incorporation of 5% of catalyst. For all these features above mentioned, we envision that transamidation could gain space in *vitrimer* science as a new exchange reaction and could be applied in the thermosets field to reduce their environmental impact.

4 | EXPERIMENTAL SECTION

4.1 | Materials

Oleic acid (90%), trimethylorthoformate (99%), sulfuric acid (99%), methanol (99%), tetrafluoroboric acid diethyl ether complex (57% in Et_2O), 1-Methylimidazole (99%), tris(2-aminoethyl)amine (96%), boric acid (99%), *m*-chloroperbenzoic acid (77%), $NaHCO_3$ (99%), Na_2SO_4

(99%), dichlorometane (99%), tetrahydrofuran (99%), flash silica (High-purity grade) and silica gel on TLC plates (5 cm × 20 cm, silica gel matrix, fluorescent indicator) were purchased from Sigma Aldrich Co. and used without further purification.

4.2 | Synthesis of methyl oleate

Oleic acid (20.0 g; 0.0700 mol), trimethylorthoformate (2.80 ml; 0.0250 mol), methanol (20.0 ml; 0.490 mol) and sulfuric acid (0.600 ml; 0.011 mol) were mixed in a round-bottomed flask and heated to reflux for 6 h while stirring with a magnetic stir bar.[43] The reaction mixture was diluted with diethyl ether and then washed with water, brine and lastly 10 wt.% Na_2CO_3 aqueous solution to remove acid residue. The organic fraction was dried over anhydrous Na_2SO_4 and filtered, and the solvent was removed in a rotary evaporator.

Reaction yield: 98%

^{1}H NMR (400 MHz, $CDCl_3$, δ): 5.36–5.32 (m, 2H; —CH═CH—), 3.66 (s, 3H; —OCH_3), 2.30 (t, $J = 8$ Hz, 2H; —CH_2—CO—), 2.04–1.97 (m, 4H; —CH_2—CH═CH—CH_2—), 1.66–1.57 (m, 2H; —CH_2—CH_2—CO—), 1.37–1.24 (m, 20H; —CH_2—), 0.87 (t, $J = 8$ Hz, 3H; —CH_3).

^{13}C NMR (100 MHz, $CDCl_3$, δ): 174.0 (—COO—), 130.1 (—CH═CH—), 64.3 (CH_3—OCO—), 34.5–22.8 (—CH_2—), 14.2 (—CH_3).

4.3 | Synthesis of epoxidized methyl oleate

Methyl Oleate was weighted in a round-bottomed flask (3.64 g; 0.0120 mol). Dichloromethane (50.0 ml) was added and the mixture was stirred using a magnetic stir bar and cooled in a 0°C ice/water bath. *m*-Chloroperbenzoic acid (3.18 g; 0.0180 mol) was slowly added over 5 min, the ice bath is then removed, and the reaction is allowed to stir for 3 h. The reaction mixture was washed with an aqueous saturated solution of Na_2SO_3 to remove the excess of *m*-CPBA (until potassium iodide starch test paper showed no color) and with a 10 wt.% Na_2CO_3 aqueous solution. The organic fraction was dried over anhydrous Na_2SO_4 and filtered, then the solvent was removed in a rotary evaporator. The crude product was then isolated by filtering through silica with a $10\%_{v.v.}$ diethyl ether/hexane eluent solution. Eventually, the solvent was removed by rotary distillation under vacuum.

Reaction yield: 98%

^{1}H NMR (400 MHz, $CDCl_3$, δ): 3.66 (s, 3H; —OCH_3), 2.30 (t, $J = 8$ Hz, 2H; —CH_2—CO—), 2.82–2.94 (m, 2H; —CH—O—CH—), 1.57–1.66 (m, 2H; —CH_2—CH_2—CO—), 1.43–1.51 (m, 4H; —CH_2—CH—O—), 1.23–1.36 (m, 20H; —CH_2—), 0.87 (t, $J = 8$ Hz, 3H; —CH_3).

^{13}C NMR (100 MHz, $CDCl_3$, δ): 174.0 (—COO—), 64.2 (CH_3—OCO—), 57.5 (—CH—O—CH—), 34.5–22.8 (—CH_2—), 14.2 (—CH_3).

IR (ATR), $\nu = 1738$ cm^{-1} (C═O stretch), 1212 (epoxide ring-breathing), 845 and 824 (epoxide symmetric stretch).

4.4 | Synthesis of 1-methylimidazolium tetrafluoroborate

1-Me Imidazole (400 mg; 2.43 mmol) was weighted in a vial and then stirred and cooled to 0 °C in an ice/water bath.[36] Tetrafluoroboric acid diethyl ether complex (394 mg; 2.43 mmol) was then slowly added over a period of 30 min and the reaction was left stirring for 2 h. The solvent was then removed by vacuum evaporation.

4.5 | Epoxide opening and synthesis of polymer network

Epoxidized methyl oleate (300 mg, 0.960 mmol), tris (2-aminoethyl)amine (143 mg; 0.960 mmol), 1-Me-Imidaziolium tetrafluoroborate (10.0 mg, 0.0600 mmol), and different amount of $B(OH)_3$ (0, 2, 5, and 10 mol%, corresponding to 0, 0.27, 0.67, 1.34 wt.% respectively) were mixed in a vial and heated at 100°C for 4 h under stirring and argon flux. The obtained homogeneous solution was, then, cured at 120°C for 20 h. The vial was then cooled to room temperature and the polymer removed. The sample were named EMO-TREN *x%*, where *x%* is the $B(OH)_3$ concentration, expressed as mol %.

4.6 | NMR and ATR-FTIR analysis

^{1}H and ^{13}C NMR spectra were recorded in $CDCl_3$ on a Bruker AVANCE-400 operating at 400.13 MHz and 100.61 MHz, respectively.

FT-IR spectra in attenuated total reflection mode (ATR) were acquired by using a Thermo Nicolet 6700 instrument (Thermo Scientific, MA), equipped with a Golden Gate diamond single reflection device (Specac LTD, England). The spectra were collected co-adding 200 scans at a resolution of 4 cm^{-1} in the range 4000–600 cm^{-1}.

4.7 | Swelling tests

Weighted polymer samples (w_0) were immersed in tetrahydrofuran for 48 h at room temperature. After that

period of time, the samples were withdrawn, the excess of solvent on the surface removed and weighted (w_1). Then, the swelled samples were dried and weighted again (w_2). Gel fraction (GF) and swelling ratio (SR) were calculated by using the equations $GF = \frac{w_2}{w_0}$ and $SR = \frac{(w_1 - w_2)}{w_2}$, respectively.

4.8 | Thermogravimetric analysis (TGA) and different scanning calorimetry (DSC)

The thermal stability of the obtained EMO-TRENs was investigated by thermogravimetric analysis (TGA), using a Mettler TG 50 thermobalance equipped with a Mettler TC 10 A processor. All measurements were carried out under nitrogen flow from 25 to 500°C, at a heating rate of 10°C min^{-1}.

The thermal properties of the polymers were characterized by DSC (Mettler Toledo DSC 822^e), heating at 10°C min^{-1} about 5 mg of sample from −50 to 180°C.

The results of the analysis are reported as average values ± standard deviations on at least three experiments conducted on different samples.

4.9 | Dynamic mechanical analysis (DMA)

Dynamic mechanical thermal analyses (DMTA) were carried out in compression mode using a Rhemoetrics Solid Analyzer RSA II on 3 × 3 × 3 mm^3 specimens. The real (E') and imaginary (E'') components of the complex compression modulus as well as tan δ were investigated by heating the sample at 3°C min^{-1} from 30 to 150°C. A test frequency of 1 Hz and 0.01% dynamic deformation were employed. Stress relaxation experiments were carried out at different temperatures, chosen in the sample rubbery plateau, and by applying a constant stress of 1 KPa.

4.10 | Tensile tests

The mechanical properties of the as prepared and the reprocessed EMO-TRENs were analyzed by tensile stress–strain experiment performed with an INSTRON 4502, equipped by a 2 kN load cell, at a crosshead speed of 5 mm/min. The dumbbell specimens were prepared by polymerizing EMO-TRENs in a Teflon mold. Specifically, the size of C-type die of ASTM D 412 method was reduced by about a 0.5 factor to accommodate the mold in the reaction vessel, resulting in an overall length of 51 mm and a narrow section of 3 mm wide and 18 mm long. The thickness of the specimens was about 2 mm. After the test and the sample break, the two sample portions were inserted in the mold, taking care that the two surfaces of fracture were in contact, and heated at 140°C for 120 min. Then, the healed samples were subjected to a second stress–strain experiment in the same condition used for the pristine ones.

All the results of the mechanical characterization are reported as average values ± standard deviations on at least three experiments conducted on different samples.

4.11 | Reprocessability tests

Reprocessability test was conducted by pressing small fragments of the selected EMO-TREN 5% sample in a hot press heated to 140°C, for 3 h, under a pressure of 98 MPa. The obtained films, about 0.4 mm thick, were die-cut in dumbbell shaped specimens with the narrow section of 3 mm width and 10 mm length of. After the mechanical characterization, the broken samples underwent a second reprocessing stage for new stress–strain experiments. The mechanical tests were carried in triplicate by using the same conditions previously described. The results are reported as average values ± standard deviations.

ACKNOWLEDGMENT

Open Access Funding provided by Universita degli Studi di Roma La Sapienza within the CRUI-CARE Agreement.

AUTHOR CONTRIBUTIONS

Luca Pettazzoni: Conceptualization (lead); investigation (equal); project administration (lead); writing – original draft (equal); writing – review and editing (equal). **Francesca Leonelli:** Supervision (lead); writing – review and editing (equal). **Andrea Martinelli:** Data curation (equal); supervision (lead); writing – original draft (equal); writing – review and editing (equal). **Luisa Maria Migneco:** Writing – review and editing (equal). **Sara Alfano:** Data curation (equal); investigation (equal); writing – original draft (equal). **Daniele Di Luca:** Investigation (equal); writing – original draft (equal); writing – review and editing (equal). **Lorenzo Celio:** Data curation (equal); software (equal); writing – original draft (equal); writing – review and editing (equal). **Valerio Di Lisio:** Data curation (supporting); investigation (equal).

DATA AVAILABILITY STATEMENT

The data that support the findings of this study are available from the corresponding author upon reasonable request.

ORCID

Luca Pettazzoni https://orcid.org/0000-0002-6580-2675

REFERENCES

[1] A. P. Da Costa, E. C. Botelho, M. L. Costa, N. E. Narita, J. R. Tarpani, *J. Aereosp. Technol. Manag.* **2012**, *4*, 255.
[2] T. Vidil, F. Tournilhac, S. Musso, A. Robisson, L. Leibler, *Prog. Polym. Sci.* **2016**, *62*, 126.
[3] D. J. Fortman, J. P. Brutman, C. J. Cramer, M. A. Hillmyer, W. R. Dichtel, *J. Am. Chem. Soc.* **2015**, *137*, 14019.
[4] C. J. Kloxin, T. F. Scott, B. J. Adzima, C. N. Bowman, *Macromolecules* **2010**, *43*, 2643.
[5] W. Denissen, J. M. Winne, F. Du Prez, *Chem. Sci.* **2016**, *7*, 30.
[6] M. K. McBride, B. T. Worrell, T. Brown, L. M. Cox, N. Sowan, C. Wang, M. Podgoroski, A. M. Martinez, C. N. Bowman, *Annu. Rev. Chem. Biomol. Eng.* **2019**, *10*, 175.
[7] X. Chen, M. A. Dam, K. Ono, A. Mal, H. Shen, S. R. Nutt, K. Sheran, F. A. Wudl, *Science* **2002**, *295*, 1698.
[8] Y. Higaki, H. Otsuka, A. Takahara, *Macromolecules* **2006**, *39*, 2121.
[9] R. Martin, A. Rekondo, A. R. De Luzuriaga, G. Cabañero, H. J. Grande, I. Odriozola, *J. Mater. Chem. A* **2014**, *2*, 5710.
[10] B. Zhang, Z. A. Digby, J. A. Flum, P. Chakma, J. M. Saul, J. L. Sparks, D. Konkolewicz, *Macromolecules* **2016**, *49*, 6871.
[11] H. Ying, Y. Zhang, J. Cheng, *Nat. Commun.* **2014**, *5*, 3218.
[12] T. F. Scott, A. D. Schneider, W. D. Cook, C. N. Bowman, *Science* **2005**, *308*, 1615.
[13] Y. Amamoto, J. Kamada, H. Otsuka, A. Takahara, K. Matyjaszewski, *Angew. Chem. Int. Ed.* **2011**, *50*, 1660.
[14] R. Nicolaÿ, J. Kamada, A. Van Wassen, K. Matyjaszewski, *Macromolecules* **2010**, *43*, 4355.
[15] D. Montarnal, M. Capelot, F. Tournilhac, L. Leibler, *Science* **2010**, *334*, 965.
[16] P. Taynton, K. Yu, R. K. Shoemaker, Y. Jin, H. J. Qi, W. Zhang, *Adv. Mater.* **2014**, *26*, 3938.
[17] S. Dhers, G. Vantomme, L. Avérous, *Green Chem.* **2019**, *21*, 1596.
[18] Y. Xu, K. Odelius, M. Hakkarainen, *ACS Sustain. Chem. Eng.* **2020**, *8*, 17272.
[19] Y. X. Lu, F. Tournilhac, L. Leibler, Z. Guan, *J. Am. Chem. Soc.* **2012**, *134*, 8424.
[20] T. B. Worrel, M. K. McBride, G. B. Lyon, L. M. Cox, C. Wang, S. Mavila, C. H. Lim, H. M. Coley, C. B. Musgrave, Y. Ding, C. N. Bowman, *Nat. Commun.* **2018**, *9*, 2804.
[21] P. Yan, W. Zhao, X. Fu, Z. Liu, W. Kong, C. Zhou, J. Lei, *RSC Adv.* **2017**, *7*, 26858.
[22] D. W. Lee, H. N. Kim, D. S. Lee, *Molecules* **2019**, *24*, 1.
[23] W. Denissen, G. Rivero, R. Nicolaÿ, L. Leibler, J. M. Winne, F. Du Prez, *Adv. Funct. Mater.* **2015**, *25*, 2451.
[24] A. Ruiz De Luzuriaga, R. Martin, N. Markaide, A. Rekondo, G. Cabañero, J. Rodriguez, I. Odriozola, *Mater. Horizons* **2016**, *3*, 241.
[25] C. Di Mauro, S. Malburet, A. Graillot, A. Mija, *ACS Appl. Bio Mater.* **2020**, *3*, 8094.
[26] R. L. Snyder, D. J. Fortman, G. X. De Hoe, M. A. Hillmyer, W. R. Dichtel, *Macromolecules* **2018**, *51*, 389.
[27] A. Khan, N. Ahmed, M. Rabnawaz, *Polymers* **2027**, *2020*, 12.
[28] Y. H. Chu, Y. L. Kung, *Food Chem.* **1998**, *62*, 191.
[29] K. M. Moore, D. A. Knauft, *J. Hered.* **1989**, *80*, 252.
[30] N. H. Muhamad Gh, J. Gimbun, S. Nurdin, *J. Appl. Sci.* **2014**, *14*, 1425.
[31] T. X. Nguyenthi, J. P. Bazile, D. Bessières, *Energies* **2018**, *11*, 1212.
[32] D. Swern, W. E. Parker, *J. Am. Oil Chem. Soc.* **1952**, *29*, 431.
[33] C. D. Amorim, A. G. Camilo, C. de Oliveira, M. E. Petenucci, G. G. Fonseca, *Sustain. Mater. Technol.* **2015**, *6*, 9.
[34] R. Elkacmi, N. Kamil, M. Bennajah, S. Kitane, *Biomed Res. Int.* **2016**, *2016*, 9.
[35] S. Kumar, S. Negi, *3 Biotech.* **2015**, *5*, 847.
[36] M. I. Loizides, X. I. Loizidou, D. L. Orthodoxou, D. Petsa, *Recycling* **2019**, *4*, 16.
[37] B. Atanu, B. K. Sharma, K. M. Doll, S. Z. Erhan, J. L. Willett, H. N. Cheng, *J. Agric. Food Chem.* **2009**, *57*, 8136.
[38] T. B. Nguyen, J. Sorres, M. Q. Tran, L. Ermolenko, A. Al-Mourabit, *Org. Lett.* **2012**, *14*, 3202.
[39] D. Radojčić, J. Hong, M. Ionescu, X. Wan, I. Javni, Z. S. Petrović, *Eur. J. Lipid Sci. Technol.* **2016**, *118*, 1507.
[40] D. Peak, G. W. Luther III., D. L. Sparks, *Geochim. Cosmochim. Acta* **2003**, *67*, 2551.
[41] Y. Wen, Y. Lu, H. Xiao, X. Qin, *Mater. Des.* **2012**, *36*, 728.
[42] Z. Liu, C. Yu, C. Zhang, Z. Shi, J. Yin, *ACS Macro Lett.* **2019**, *8*, 233.
[43] L. Montero De Espinosa, A. Gevers, B. Woldt, M. Graß, M. A. R. Meier, *Green Chem.* **1883**, *2014*, 16.

How to cite this article: L. Pettazzoni, F. Leonelli, A. Martinelli, L. M. Migneco, S. Alfano, D. Di Luca, L. Celio, V. Di Lisio, *J. Appl. Polym. Sci.* **2022**, e52408. https://doi.org/10.1002/app.52408